

## From deep inelastic scattering to photoproduction: A unified approach

G. Kerley and G. Shaw

*Department of Physics and Astronomy, Schuster Laboratory, University of Manchester, Manchester M13 9PL, United Kingdom*

(Received 21 July 1997)

The strikingly different high energy behaviors of real photoabsorption cross sections with  $Q^2=0$  and the low  $x$  proton structure function at large  $Q^2$  are studied from a laboratory frame viewpoint, in which the  $x$  and  $Q^2$  dependence reflects the space-time structure of the interaction. This is done using a simple model which incorporates hadron dominance, but attributes the striking enhancement observed at DESY HERA at very low  $x$  and high  $Q^2$  to contributions from heavy long-lived fluctuations of the incoming photon. Earlier published predictions of the model for the then unknown behavior of the structure function at small  $x$  and intermediate  $Q^2$  are shown to be strikingly confirmed by recent experimental data. A simultaneous analysis of real photoabsorption data and structure function data for  $0 \leq x < 0.1$  and  $0 \leq Q^2 \leq 15 \text{ GeV}^2$  is then reported. An excellent fit is obtained, with all parameters in the restricted ranges allowed by other physical requirements. [S0556-2821(97)02523-X]

PACS number(s): 13.60.Hb, 12.40.Vv, 13.60.-r

### I. INTRODUCTION

At high energies, the real photoabsorption cross section

$$\sigma_{\gamma p}(\nu, Q^2=0) \approx a_P \nu^{\alpha_P-1} + a_R \nu^{\alpha_R-1}$$

is characterized by the intercept  $\alpha_P \approx 1.08$  of the ‘‘soft’’ Pomeron familiar from hadron scattering [1], together with an effective contribution from lower-lying Regge trajectories with  $\alpha_R \approx 0.55$ . The same behavior characterizes the proton structure function in the intermediate  $x$  region  $0.02 \leq x \leq 0.1$ , but experiments at the DESY  $ep$  collider HERA [2,3] in 1993 first observed the much sharper rise in the structure function at small  $x < 0.02$  and large  $Q^2 > 8 \text{ GeV}^2$  associated with the ‘‘hard’’ Pomeron. Here we focus on the transition between these contrasting behaviors in the intermediate  $Q^2$  region  $0 < Q^2 < 8 \text{ GeV}^2$  using an approach suggested by one of us [4]. This was used to predict the behavior at intermediate  $Q^2$  in 1994 [5], but there was no data with which to confront the predictions. Subsequently the experimental situation has been transformed by precise data both at high  $Q^2$  and in the hitherto unexplored region of low  $x$  and intermediate  $Q^2$  [6–8]. Here we examine whether the new data at intermediate  $Q^2$  agree with the prior predictions of the model, and whether its greater precision and its extension to smaller  $x$  values enable the intercept of the hard Pomeron to be determined more precisely by the data.

The model used is described in the next section. However, it will be useful to first summarize the underlying approach [4]. This adopts the laboratory frame viewpoint typical of hadron dominance models, and emphasizes the role of the coherence length

$$l = \frac{2\nu}{m^2 + Q^2} = \frac{1}{Mx} \frac{1}{1 + m^2/Q^2} > \frac{1}{Mx}, \quad (1)$$

which represents the typical distance traveled by a vacuum fluctuation of the photon of mass  $m$ . Our assumptions on the nature of the dominant states at different coherent lengths are summarized in Fig. 1. At short coherence lengths  $l < l_0 \approx 1$

fm, corresponding to large  $x$  values  $x > 0.1$ , we assume that these states are essentially bare  $\bar{q}q$  pairs and a hadronic component of the photon has not developed. At moderate coherence lengths, they are assumed to have the single-hadron-like behavior expected for constituent  $\bar{q}q$  pairs or vector mesons. However, at very long coherence lengths, the photon fluctuations can eventually develop into the hadronic final states observed in  $e^+e^-$  annihilations.<sup>1</sup> For low masses, these states can be approximated by a sum of vector mesons, but for high masses complicated jetlike final states are observed. The idea is that the new phenomena at very small  $x$  are associated with complicated jetlike states which only play a role for masses  $m$  and coherence lengths  $l$  which are greater than some critical values  $m > m_J$  and  $l > l_C$ . By Eq. (1) this implies that they are confined to energies

$$\nu > \nu_C \equiv m_J^2 l_C / 2 \quad (Q^2=0) \quad (2)$$

in photoproduction and to the kinematic region

$$x < x_C(Q^2) \equiv \frac{1}{Ml_C} \frac{Q^2}{Q^2 + m_J^2} \quad (3)$$

for structure functions. The remaining states with  $m < m_J$  and/or  $l < l_C$  will completely dominate outside this region. They are included using conventional hadron dominance ideas which emphasize the link between real and virtual photons and provide a natural framework for describing the onset of scaling in the region<sup>2</sup>  $x_C < x < 0.1$ . For example, they

<sup>1</sup>For an attempt to understand the role of the coherence length from a more fundamental dynamical viewpoint, see Del Duca, Brodsky, and Hoyer [9].

<sup>2</sup>In hadron dominance models which give approximate scaling, the bulk of the contributions for a given  $Q^2$  comes from intermediate states with  $0 < m^2 < n Q^2$ , with  $n$  a small integer. The average value is of order  $m^2 \approx Q^2$ , for which the coherence length  $l \approx 1/2Mx$  by (1).

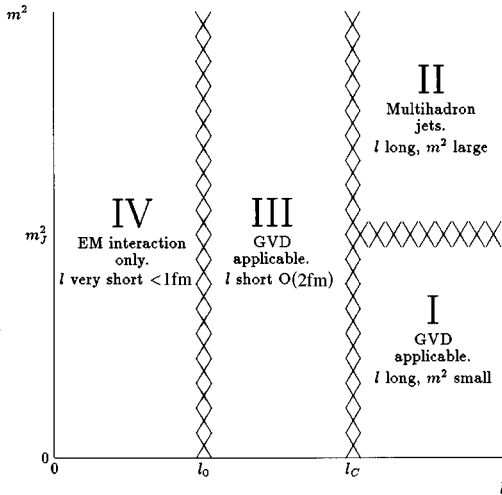


FIG. 1. Hadronic behavior of the photon for different values of the coherence length  $l$  and invariant mass squared  $m^2$  of the photon fluctuations, where  $l = 1/2Mx$  for  $m^2 = Q^2$ . Here  $l_c$  and  $M_J$  are the critical values of the coherence length and fluctuation mass that separate the two types of hadronic behavior. Another critical coherence length  $l_0 \approx 1$  fm separates the hadronic and purely electromagnetic behavior.

give a good description of the transition between real photoabsorption and deep inelastic scattering data on protons in the intermediate  $x$  region  $0.02 \leq x \leq 0.1$  [4,10], and they successfully predict the observed shadowing behavior for real photoabsorption and deep inelastic scattering on nuclei in the same  $x$  region [11–13].

## II. SIMPLE MODEL

In the hadron dominance model,<sup>3</sup> the total cross section for photoabsorption is given by an expression of the form

$$\sigma_{\gamma p}(\nu, Q^2) = \int dm^2 \int dm'^2 \frac{\rho(m, m', s)}{(m^2 + Q^2)(m'^2 + Q^2)}, \quad (4)$$

corresponding to Fig. 2. Conventional hadron physics and duality with the parton model both require large “diagonal”  $m = m'$  and large “off-diagonal”  $m \neq m'$  components to be present, and the latter must be explicitly incorporated if the approximate scaling behavior of the shadowing for deep inelastic scattering on heavy nuclei is to be understood [11–13]. However, these off-diagonal contributions are dominated by terms in which the two mass values  $m$  and  $m'$  are not very different. Equation (4) is therefore often replaced by a simple diagonal approximation

$$\sigma_{\gamma p}(\nu, Q^2) = \int_{m_0^2}^{\infty} dm^2 \frac{\rho(\nu, m^2)}{(m^2 + Q^2)^2}, \quad (5)$$

where  $\rho(\nu, m^2)$  is an effective quantity, meant to represent

<sup>3</sup>For reviews, see, for example, [4] and [14] and references therein.

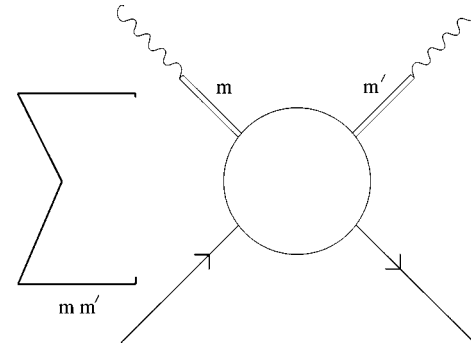


FIG. 2. The hadron dominance model (4).

the more complicated structure on average.<sup>4</sup> Single-hadron-like behavior of the intermediate states can be incorporated by assuming a Regge-type energy dependence

$$\rho^P(\nu, m^2) = f_P(m^2) \nu^{\alpha_P - 1}$$

for the dominant diffractive contribution, where  $f_P(m^2)$  is a smoothly varying function of mass chosen to lead to approximate scaling at large  $Q^2$ . In particular, if we assume

$$\rho^P(\nu, m^2) = a \nu^{\alpha_P - 1} (m^2)^{1 - \alpha_P}, \quad (6)$$

this gives

$$F_2^P = Ax \nu^{\alpha_P} \int_{m_0^2}^{\infty} dm^2 \frac{(m^2)^{1 - \alpha_P}}{(m^2 + Q^2)^2} \quad (7)$$

for the soft Pomeron contribution to the structure function, where

$$A = \frac{Ma}{2\pi^2\alpha}.$$

This formula obviously embodies single-hadron-like behavior  $\alpha_P \approx 1.08$  for all intermediate states. Here we modify it by adjusting the contributions from  $m > m_J$  and  $l > l_c$ , which is meant to roughly characterize the region in which single-hadron-like behavior has given way to a more complicated behavior. This behavior is unknown, and so we parametrize it by the simplest possible generalization of Eq. (6), in which  $A$  and  $\alpha_P$  are replaced by new parameters  $\tilde{A}$  and  $\alpha'_P$  to allow for a different magnitude and energy dependence. In this way we arrive at a representation of the form

<sup>4</sup>If Eq. (5) were exact, in the context of scaling in  $e^+ e^-$  annihilation and deep inelastic scattering it would imply that the total cross sections  $\sigma_m$  for states  $m$  scattering on nucleons decreased approximately as  $m^{-2}$ . This counterintuitive result is sometimes known as the Gribov paradox. It implies that the mean free paths in nuclear matter increase like  $m^2$ , so that shadowing would die away at large  $Q^2$  at fixed  $x$ . These problems do not occur in “off-diagonal models” of the form (5), when the effective quantity  $\rho(\nu, m^2)$  results from destructive interference between diagonal and off-diagonal terms in Eq. (4). (Again, see [4,12,14] and references therein.)

$$\begin{aligned}
F_2^P &= Ax\nu^{\alpha_P} \int_{m_0^2}^{\infty} dm^2 \frac{(m^2)^{1-\alpha_P}}{(m^2+Q^2)^2} [\theta(m_J^2-m^2) \\
&\quad + \theta(m^2-m_J^2)\theta(l_C-l)] \\
&\quad + \tilde{A}x\nu^{\alpha'_P} \int_{m_0^2}^{\infty} dm^2 \frac{(m^2)^{1-\alpha'_P}}{(m^2+Q^2)^2} \theta(m^2-m_J^2)\theta(l-l_C).
\end{aligned} \tag{8}$$

For data fits, this is conveniently rewritten as

$$\begin{aligned}
F_2^P &= \theta(m_C^2-m_J^2) \left[ Ax\nu^{\alpha_P} \int_{m_0^2}^{m_J^2} dm^2 \frac{(m^2)^{1-\alpha_P}}{(m^2+Q^2)^2} \right. \\
&\quad + \tilde{A}x\nu^{\alpha'_P} \int_{m_J^2}^{m_C^2} dm^2 \frac{(m^2)^{1-\alpha'_P}}{(m^2+Q^2)^2} \\
&\quad + Ax\nu^{\alpha_P} \int_{m_C^2}^{\infty} dm^2 \frac{(m^2)^{1-\alpha_P}}{(m^2+Q^2)^2} \left. \right] \\
&\quad + \theta(m_J^2-m_C^2) \left[ Ax\nu^{\alpha_P} \int_{m_0^2}^{\infty} dm^2 \frac{(m^2)^{1-\alpha_P}}{(m^2+Q^2)^2} \right], \tag{9}
\end{aligned}$$

where the integrals can be conveniently approximated by rapidly convergent series, as shown in the Appendix, and the critical coherence length is replaced by an effective critical mass,

$$m_C^2(x, Q^2) \equiv Q^2 \left( \frac{1}{xM_p l_C} - 1 \right), \tag{10}$$

which, unlike  $m_J^2$  (and  $l_C$ ), depends on  $Q^2$  and  $x$ . The real photon equivalent is

$$\begin{aligned}
\sigma_{\gamma p}^P(\nu, 0) &= \theta(2\nu/l_C - m_J^2) \{ B\nu^{\alpha_P-1} [(m_0^2)^{-\alpha_P} - (m_J^2)^{-\alpha_P}] \\
&\quad + C\nu^{\alpha'_P-1} [(m_J^2)^{-\alpha'_P} - (2\nu/l_C)^{-\alpha'_P}] \\
&\quad + B\nu^{\alpha_P-1} (2\nu/l_C)^{-\alpha_P} \} \\
&\quad + \theta(m_J^2 - 2\nu/l_C) [B\nu^{\alpha_P-1} (m_0^2)^{-\alpha_P}], \tag{11}
\end{aligned}$$

where

$$B \equiv \frac{2\pi^2\alpha}{2.568M_p} \frac{A}{\alpha_P}, \quad C \equiv \frac{2\pi^2\alpha}{2.568M_p} \frac{\tilde{A}}{\alpha'_P}, \tag{12}$$

and the numerical coefficients are chosen to give the cross section in mb for masses in GeV.

In addition to the contributions associated with the hard and soft Pomerons, there is also an additional contribution associated with lower-lying Regge poles. This is a small correction in the region we are considering, and we incorporate it using the simple empirical form

$$F_2^R(x, Q^2) = A_R x^{1-\alpha_R} \left( \frac{Q^2}{Q^2 + a_R} \right)^{\alpha_R}, \tag{13}$$

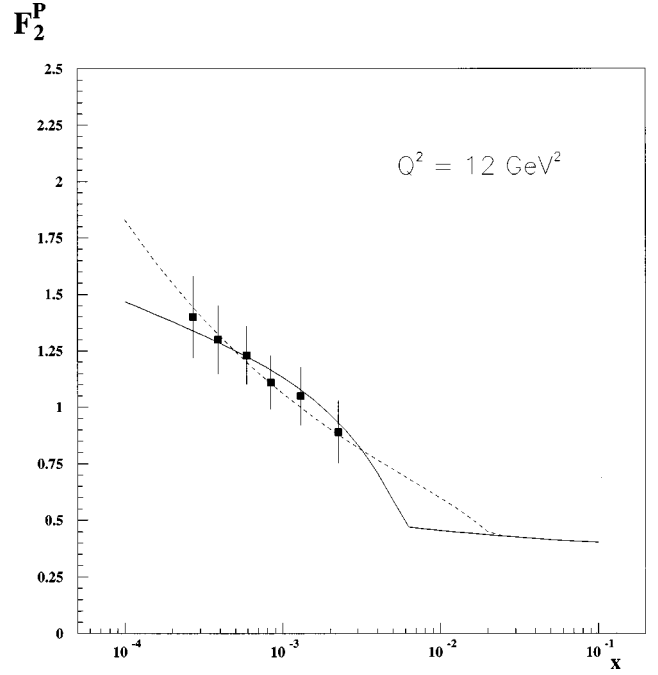


FIG. 3. The 1994 fits [5] to the 1994 H1 data [16] at  $Q^2 = 12$  GeV<sup>2</sup>, for the values  $\alpha'_P = 1.27$  (dashed line) and  $\alpha'_P = 1.08$  (solid line).

proposed by Donnachie and Landshoff [15], with the Regge intercept  $\alpha_R = 0.55$ . The total structure function is then given by

$$F_2(x, Q^2) = F_2^P + F_2^R. \tag{14}$$

In the ‘‘pre-HERA’’ regions  $\nu < \nu_C$  ( $Q^2 = 0$ ) and  $x > x_C(Q^2)$ , Eq. (9) reduces to the simpler form (7), and our parametrization (14) can be made numerically almost identical to the empirical Donnachie-Landshoff parametrization [15], which is known to give an excellent fit to photoproduction data and to structure function data in the intermediate region  $0.1 > x > 0.01$ . Correspondingly, data in this region effectively determine the parameters  $A$ ,  $m_0$ ,  $A_R$ , and  $a_R$  in Eqs. (9) and (13). The additional parameters  $\tilde{A}$ ,  $\alpha'_P$ ,  $m_J$ , and  $l_C$  in Eq. (9) describe the behavior at very small  $x$ , with  $m_J$  and  $l_C$  constrained to be a few GeV and a few Fermi, respectively.

### III. PREDICTIONS AT INTERMEDIATE $Q^2$

In 1994 [5], the parameters  $A$ ,  $m_0$ ,  $A_R$ , and  $a_R$  were fixed by fitting the simple representation, Eqs. (7), (13), and (14) to the ‘‘pre-HERA’’ data on real photoabsorption and the structure function at intermediate  $x$  values  $0.02 < x < 0.1$ . The additional parameters  $\tilde{A}$ ,  $\alpha'_P$ ,  $m_J$ , and  $l_C$  in the final form (9) were then determined by extending the fit to include the then recently available H1 data [16] at small  $x$  and large  $Q^2 > 8$  GeV<sup>2</sup> and used to predict the behavior at intermediate  $Q^2$  ( $0 < Q^2 < 8$  GeV<sup>2</sup>), where no data existed. In particular, the dramatic rise at small  $x$  observed at high  $Q^2$  was predicted to decrease rapidly and shift towards  $x=0$  as  $Q^2$  becomes smaller. In this short section, we compare these predictions

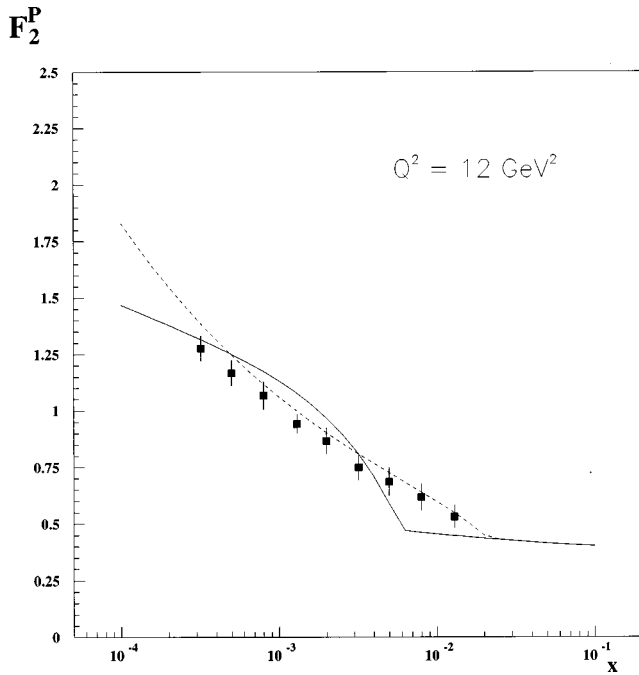


FIG. 4. Comparison of the 1994 fits [5] with the 1996 H1 data [6] at  $Q^2=12$  GeV $^2$ . The curves again correspond to  $\alpha'_p=1.27$  (dashed line) and  $\alpha'_p=1.08$  (solid line).

with the subsequent H1 measurements [6], in order to test the validity of the model.<sup>5</sup>

Before doing this, we consider the quality of the 1994 fits for  $Q^2 > 8$  GeV $^2$ . This is illustrated in Fig. 3 for the Regge intercepts

$$\alpha_R=0.55, \quad \alpha_P=1.08, \quad (15)$$

together with both a “conventional” value  $\alpha'_p=1.27$  and a very unconventional choice  $\alpha'_p=1.08$  for the intercept of the long-lived, high mass states associated with the hard Pomeron in this approach. As can be seen, this intercept was not well determined by the existing data, because of the limited  $x$  range covered. However, the 1996 H1 data [6] are more precise and extend to smaller  $x$  values. Plotting the same curves against these new data in Fig. 4 leads to a clear preference for  $\alpha'_p=1.27$ , although there are small discrepancies between the precise new data and the fit, since the parameters of the latter were determined by data of lower accuracy.

We now compare the 1994 predictions for the intermediate  $Q^2$  region  $0 < Q^2 < 8$  GeV $^2$  with the 1996 H1 data, restricting ourselves to the case  $\alpha'_p=1.27$  in light of the previous discussion.<sup>6</sup> Since in 1994 there were no data at all in this region that could be used to help determine the param-

<sup>5</sup>Since the 1994 fits were based on the 1993 H1 data at large  $Q^2$ , we initially compare their predictions at lower  $Q^2$  to later data from the same experiment. The data from ZEUS and other experiments will be discussed explicitly in the next section.

<sup>6</sup>For  $3 \times 10^{-4} < x < 5 \times 10^{-3}$ , the predictions are insensitive to the choice of  $\alpha'_p$ , but outside this range the value 1.27 rather than 1.08 is preferred.

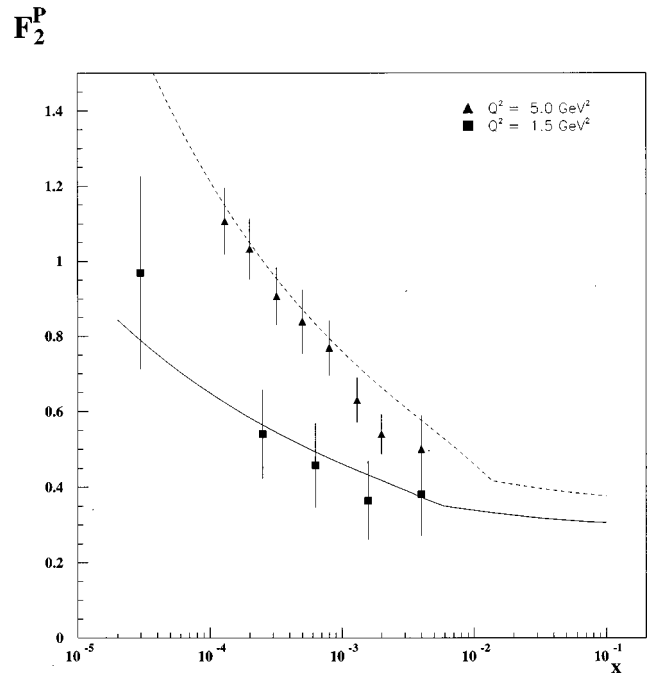


FIG. 5. Comparison of the 1994 fits [5] with the 1996 H1 data [6] at  $Q^2=1.5$  and  $5$  GeV $^2$  for  $\alpha'_p=1.27$  (dashed line).

eters of the fit, the curves shown in Fig. 5 represent a genuine prediction. When taken in conjunction with Fig. 4, they show that the  $Q^2$  dependence predicted by the model is in excellent agreement with experiment.

#### IV. GLOBAL ANALYSIS

In the last section we focused upon the 1996 H1 data at small  $x$  and intermediate  $Q^2$  because the parameters of the 1994 predictions were fixed by high  $Q^2$  data from the 1994 H1 experiment. Here we report the results of a simultaneous  $\chi^2$  fit to all the recent photoabsorption data in the wider kinematic region  $0 \leq x < 0.1$  and  $0 \leq Q^2 \leq 15$  GeV $^2$ . In doing so, we allow all the parameters in the diffractive term (9), including the Regge intercepts  $\alpha_P$  and  $\alpha'_p$ , to be determined by photoabsorption alone, in order to see whether the resulting values accord with reasonable physical expectations. However, since the nondiffractive term (13) makes only a small contribution in this region, we keep the Regge intercept fixed at the value  $\alpha_R=0.55$  obtained from hadron scattering data, leaving  $A_R$  and  $a_R$  as variable parameters.

The data used in the fit comprise the small  $x$  data of the H1 [6] and ZEUS [7] Collaborations, the small and intermediate  $x$  data of the E665 [8] Collaboration, the intermediate  $x$  data [17] of the NMC Collaboration, and the real photoabsorption cross sections [18–22]. Obviously, we need to consider the consistency of the different experiments. The ZEUS and H1 data cover a similar kinematic region, and are consistent within errors, as we shall see. In addition, for  $x \approx 0.01$

<sup>7</sup>We restrict ourselves to  $Q^2 \leq 15$  GeV $^2$  since we are interested in the transition region from real photons to deep inelastic behavior. Our simple model will of course break down eventually, since it gives exact scaling as  $Q^2 \rightarrow \infty$ .

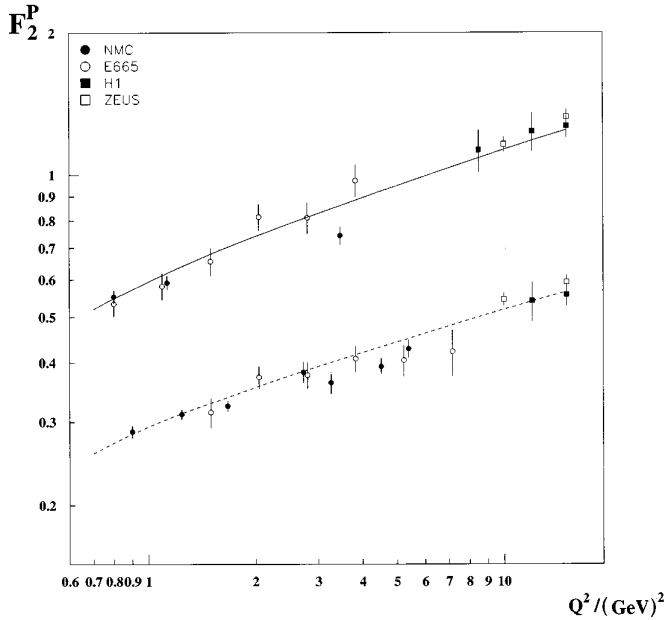


FIG. 6. Comparison of the data from various experiments at  $x=0.0125$  (lower set) and  $x=0.008$  (upper set), where the latter have been scaled by a factor of 2, for clarity. The E665 points for  $x=0.008$  have been obtained by linearly interpolating between  $x=0.007$  and  $0.009$ , and the HERA data have also been interpolated slightly from neighboring points. The dashed (solid) lines show the result of the global fit described in the text for  $x=0.0125$  ( $0.008$ ), respectively.

there is data from both E665 and New Muon Collaboration (NMC) at low and intermediate  $Q^2$ , as well as high  $Q^2$  data from ZEUS and H1. As can be seen from Fig. 6, the experiments are consistent with each other, except for the three NMC points at  $(x, Q^2) = (0.0125, 3.26)$ ,  $(0.0125, 4.52)$ , and, especially,  $(0.008, 3.47)$ .

The resulting fits to the various data sets are shown in Figs. 7–11 and the corresponding  $\chi^2$  contributions listed in Table I, where in all cases, the statistical and point systematic errors have been combined in quadrature. As can be seen, good fits are obtained for all data sets with the possible exception of the NMC data, which contributes 94 towards  $\chi^2$  from 66 data points. However, it is clear from Fig. 10 that the fit is satisfactory, except for a few points, usually towards the edge of the kinematic range of the experiment, which make a very large contribution to  $\chi^2$ . For example, the three NMC points discussed above contribute 23 towards  $\chi^2$ , and on examining Fig. 6, it is difficult to see how any smooth curve, which fits the rest of the data, can do any better.

With this small caveat, we conclude that the consistency of the data and the quality of the fit are very satisfactory. The corresponding parameter values are given in Table II together with their errors.<sup>8</sup> In addition, we have performed a series of seven fits in which one of the data sets listed in Table I is omitted, and the remaining six are fitted, in order to check whether the parameter values are sensitive to small changes in the data set. The results are summarized in Table

<sup>8</sup>These errors are, of course, correlated; the full error matrix is available on request.

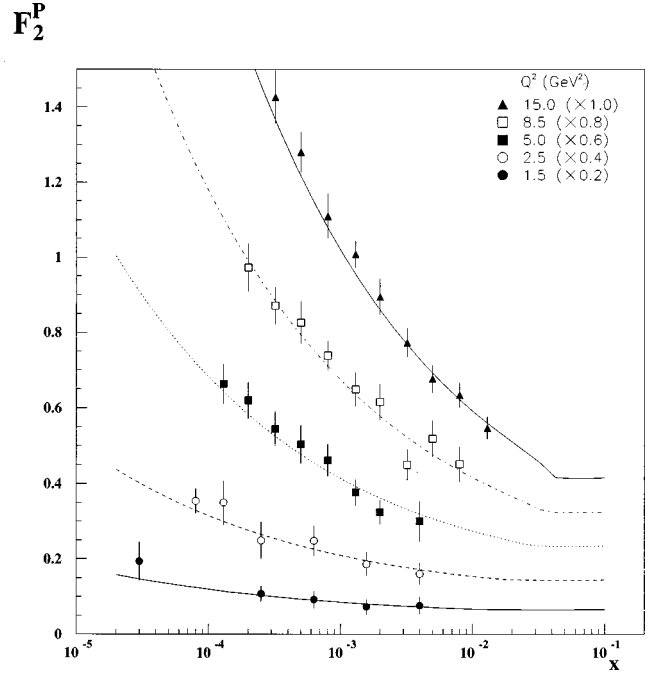


FIG. 7. Comparison of the global fit with the 1996 H1 data [6] for representative  $Q^2$  values.

III. As can be seen, the parameters are fairly stable against such changes, except for the parameters  $A_R$  and  $a_R$  associated with the small nondiffractive term (13). These are only separately well determined<sup>9</sup> if the NMC data, covering the intermediate  $x$  region, are included.

We now comment briefly on the values obtained for the

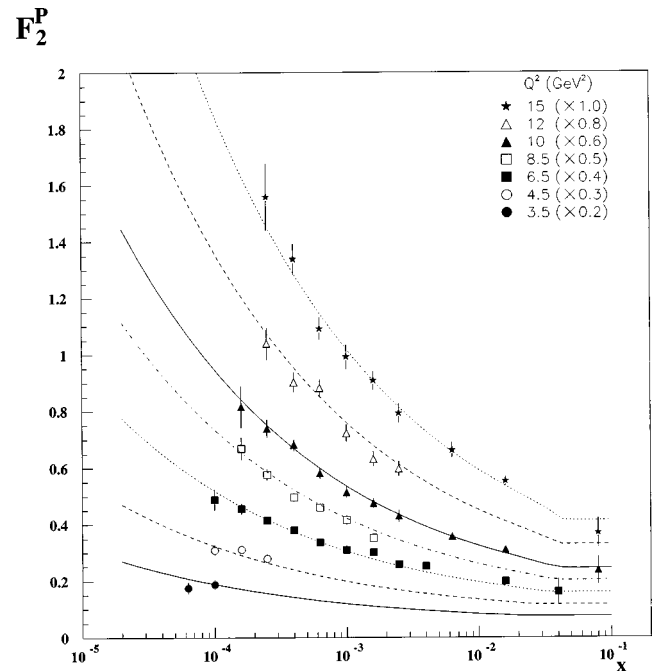


FIG. 8. Comparison of the global fit with the 1996 ZEUS data [7].

<sup>9</sup>The ratio is well determined by real photoabsorption data.

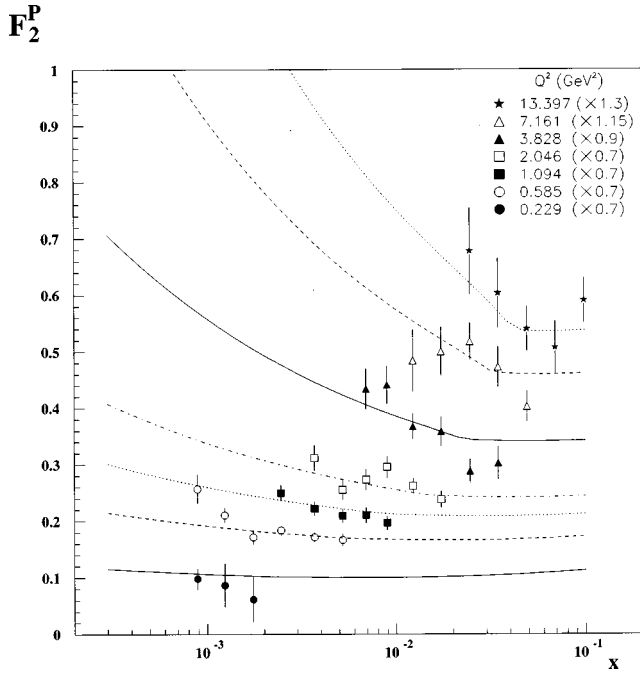


FIG. 9. Comparison of the global fit with the E665 data [8] for representative  $x$  values.

parameters. In contrast to the 1994 fits, the intercept

$$\alpha'_p = 1.289 \pm 0.007 \quad (16)$$

of the hard Pomeron is well determined, while the value

$$\alpha_p = 1.059 \pm 0.007$$

of the intercept of the soft Pomeron is similar to, but perhaps slightly lower than, the value  $\alpha_p = 1.08$  favored by the analysis of hadronic total cross sections [1] in terms of a simple Regge pole model of the Pomeron. The value

$$m_0 = 0.68 \pm 0.01$$

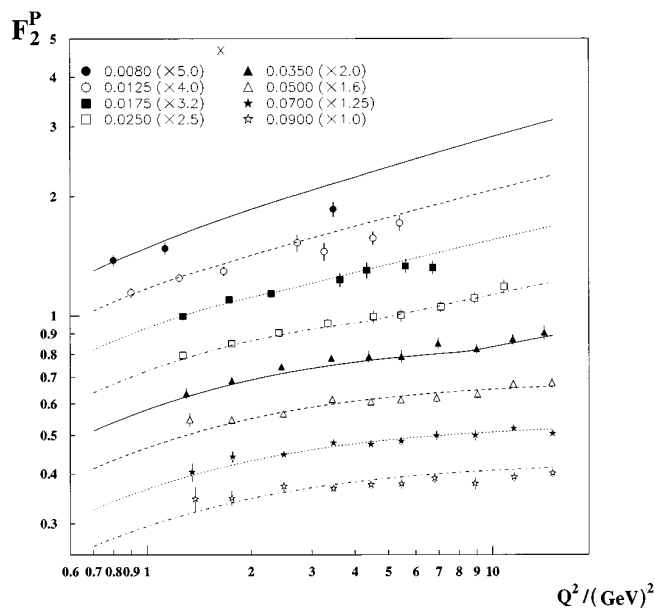


FIG. 10. Comparison of the global fit with the NMC data [17].

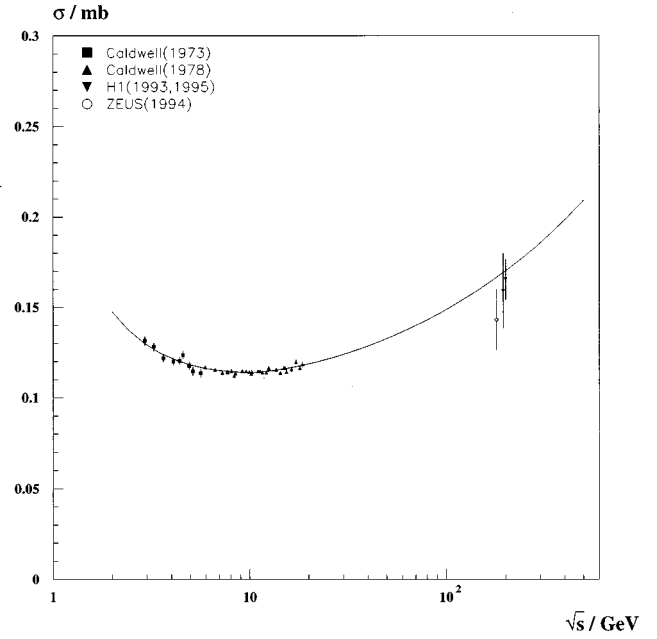


FIG. 11. Comparison of the global fit with the real photoabsorption data [18–22].

is somewhat below the  $\rho$  mass, as predicted long ago by generalized vector dominance models with off-diagonal terms,<sup>10</sup> while the value of the parameter

$$m_J = 2.51 \pm 0.02$$

corresponding to the transition from resonance dominance to jetlike behavior accords well with  $e^+ e^-$  annihilation data. Finally the value for the characteristic distance over which jetlike behavior develops for heavy states is

$$l_C = 3.45 \pm 0.06 \text{ fm.}$$

This is also very reasonable, given the usual estimate  $l \approx 1$  fm for the characteristic distance over which light  $q\bar{q}$  states develop into vector mesons, based on, for example, the onset of nuclear shadowing effects in photoproduction on nuclei.

## V. SUMMARY

We have given a unified treatment of both real and virtual photoabsorption data in terms of a modified hadron dominance model, in which the striking enhancement observed at HERA at very low  $x$  and high  $Q^2$  is attributed to contributions from heavy long-lived fluctuations of the incoming photon. We have shown that the published predictions of the model for small  $x$  and low and intermediate  $Q^2 < 8 \text{ GeV}^2$ , where no data previously existed, are confirmed by recent data, that the model gives an excellent fit to the much improved real photoabsorption and proton structure function data over the whole region  $0 \leq x < 0.1$  and  $0 \leq Q^2 \leq 15 \text{ GeV}^2$ , and that the values of the parameters of the model, determined from this real and virtual photoabsorption data alone,

<sup>10</sup>This follows naturally from the destructive interference between the diagonal and off-diagonal terms [14,23].

TABLE I. Breakdown of  $\chi^2$  into contributions from different data sets to the global fit.

Data source		Number of points	$\chi^2$
Structure function data	H1	64	35.7
	ZEUS	47	47.1
	NMC	66	93.9
	E665	77	74.0
Real photoabsorption	Caldwell'73	9	8.8
	Caldwell'78	30	33.8
	HERA	3	2.3
All data		296	295.6

are in good agreement with physical expectations and other sources of information.

### ACKNOWLEDGMENTS

We would like to thank Dr. J. Forshaw for several helpful discussions and PPARC for financial support.

### APPENDIX: EVALUATION OF INTEGRALS

Data fits were performed using the MINUIT routine to minimize  $\chi^2$  with respect to the parameters of Eq. (9). This is computationally quite involved and speed and efficiency are at a premium. For this reason the integrals in Eq. (9) were evaluated by using a convenient series expansion rather than the normal methods of numerical quadrature.

The integrals in Eq. (9) can be easily written as linear combinations of integrals of the form

$$\int_b^\infty \frac{z^{-\epsilon}}{(Q^2+z)^2} dz, \quad 0 < |\epsilon| < 1, \quad (\text{A1})$$

where the lower limits usually arise from the step functions, and can depend on  $x$  and  $Q^2$ . Writing  $Q^2 y = z$ ,

TABLE II. Parameter values and errors resulting from the global fit. (Natural units, based on the GeV, are used throughout.)

Diffractive (Pomeron)	
$m_0^2$	$0.466 \pm 0.008$
$\alpha_P$	$1.059 \pm 0.007$
$A$	$0.629 \pm 0.022$
$m_J^2$	$6.28 \pm 0.08$
$\alpha'_P$	$1.289 \pm 0.007$
$\tilde{A}$	$0.457 \pm 0.019$
$l_C$	$17.5 \pm 0.3$
Nondiffractive (Regge)	
$A_R$	$0.163 \pm 0.029$
$a_R$	$0.039 \pm 0.009$
$\alpha_R$	$0.547(\text{fixed})$

$$\int_b^\infty \frac{z^{-\epsilon}}{(Q^2+z)^2} dz = Q^{-2(1+\epsilon)} J(r, \epsilon), \quad (\text{A2})$$

where

$$J(r, \epsilon) = \int_r^\infty \frac{y^{-\epsilon}}{(1+y)^2} dy$$

and  $r = b/Q^2$ .

If  $r \geq 1$ , then

$$J(r, \epsilon) = \frac{1}{r^\epsilon} \left( \frac{1}{1+r} + \frac{\epsilon}{r} \left\{ \ln \left( \frac{1+r}{r} \right) - \frac{1}{1+\epsilon} \right\} - \epsilon \left( 1 + \epsilon \sum_{n=1}^{\infty} \frac{(-1)^{n+1}}{n(n+1+\epsilon)r^{(n+1)}} \right) \right). \quad (\text{A3})$$

If  $r < 1$ , then

TABLE III. Parameter and  $\chi^2$  values for fits with one data set in turn excluded.

	Omitted data set						
	H1	Structure function			Photoabsorption		
		ZEUS	E665	NMC	Caldwell'73	Caldwell'78	HERA
$m_0^2$	0.455	0.465	0.463	0.508	0.458	0.463	0.469
$\alpha_P$	1.054	1.059	1.055	1.067	1.049	1.050	1.064
$A$	0.628	0.628	0.638	0.655	0.654	0.653	0.617
$m_J^2$	5.823	6.497	6.303	6.277	5.945	5.911	6.339
$\alpha'_P$	1.291	1.316	1.290	1.274	1.286	1.287	1.290
$\tilde{A}$	0.432	0.410	0.454	0.490	0.458	0.455	0.451
$l_C$	13.48	16.90	17.42	11.60	17.82	17.72	17.32
$A_R$	0.170	0.164	0.155	0.012	0.137	0.138	0.176
$a_R$	0.0459	0.0402	0.0392	0.00029	0.0382	0.0334	0.0412
$\chi^2$	259	236	221	188	286	262	293
No. of points	232	249	219	230	287	266	293

$$\int_r^\infty \frac{y^{-\epsilon}}{(1+y)^2} dy = \frac{\pi\epsilon}{\sin(\pi\epsilon)} - \int_{1/r}^\infty \frac{y^\epsilon}{(1+y)^2} dy. \quad (\text{A4})$$

Hence

$$J(r, \epsilon) = \frac{\pi\epsilon}{\sin(\pi\epsilon)} - J(1/r, -\epsilon) \quad (\text{A5})$$

and the series for  $r > 1$  in Eq. (A3) can be used. These series

have two advantages ensuring speed and accuracy of computation: The series are alternating, and so, provided the number of terms is not too large in view of the numerical precision used, the error in the expansion is known and the degree of accuracy easily controllable; the expansion variable is the ratio of the integrand lower limit to  $Q^2$  and for many of the points this is sufficiently far from unity for the series to converge adequately after only a few terms. Even for a unit ratio, the convergence is not prohibitively slow.

- 
- [1] A. Donnachie and P. V. Landshoff, Phys. Lett. B **296**, 227 (1992).
- [2] H1 Collaboration, I. Abt *et al.*, Nucl. Phys. **B407**, 515 (1993).
- [3] ZEUS Collaboration, M. Derrick *et al.*, Phys. Lett. B **316**, 412 (1993).
- [4] G. Shaw, Phys. Lett. B **318**, 221 (1993).
- [5] P. Moseley and G. Shaw, Phys. Rev. D **52**, 4941 (1995).
- [6] H1 Collaboration, S. Aid *et al.*, Nucl. Phys. **B470**, 3 (1996).
- [7] ZEUS Collaboration, M. Derrick *et al.*, Z. Phys. C **72**, 399 (1996).
- [8] E665 Collaboration, M. R. Adams *et al.*, Phys. Rev. D **54**, 3006 (1996).
- [9] V. Del Duca, S. J. Brodsky, and P. Hoyer, Phys. Rev. D **46**, 931 (1992).
- [10] P. Moseley and G. Shaw, J. Phys. G **21**, 1043 (1995).
- [11] G. Shaw, Phys. Rev. D **47**, R3676 (1993).
- [12] G. Shaw, Phys. Lett. B **226**, 125 (1989).
- [13] M. Arneodo, Phys. Rep. **240**, 301 (1994).
- [14] For a review and references to the early literature on this subject, see A. Donnachie and G. Shaw in *Electromagnetic Interactions of Hadrons*, edited by A. Donnachie and G. Shaw (Plenum, New York, 1978), Vol. 2.
- [15] A. Donnachie and P. V. Landshoff, Z. Phys. C **61**, 139 (1994).
- [16] H1 Collaboration, C. Kleinwort, in *Proceedings of the International Conference on High Energy Physics*, Glasgow, Scotland, 1994, edited by P. J. Bussey and I. G. Knowles (IOP, Bristol, 1995).
- [17] NMC Collaboration, M. Arneodo *et al.*, Phys. Lett. B **364**, 107 (1995).
- [18] D. O. Caldwell *et al.*, Phys. Rev. D **7**, 1362 (1973).
- [19] D. O. Caldwell *et al.*, Phys. Rev. Lett. **40**, 1222 (1978).
- [20] H1 Collaboration, T. Ahmed *et al.*, Phys. Lett. B **299**, 374 (1993).
- [21] H1 Collaboration, S. Aid *et al.*, Z. Phys. C **69**, 27 (1995).
- [22] ZEUS Collaboration, M. Derrick *et al.*, Z. Phys. C **63**, 391 (1994).
- [23] H. Fraas, B. J. Read, and D. Schildknecht, Nucl. Phys. **B86**, 346 (1975).